Beyond guanine quartets: cation-induced formation of homogenous and chimeric DNA tetraplexes incorporating *iso*-guanine and guanine

Christopher Roberts, John C Chaput and Christopher Switzer

Background: *iso*-Guanine (*iso*-G) is the purine component of an isomeric Watson–Crick base pair that may have existed prebiotically. By comparing the abiotic molecular recognition properties of *iso*-G and its complement, *iso*-cytosine (*iso*-C), with those of genomic nucleotide bases, it may be possible to explain the exclusion of the *iso*-G–*iso*-C base pair from modern genomes. Whether a nucleobase forms quartets may have a key role in determining its functionality. Biotically, nucleic acid tetraplexes have been implicated in cellular functions; prebiotically, tetraplexes would probably interfere with replication. Recently, *in vitro* selection has yielded receptors and catalysts that incorporate G quartets. The versatility of these structures could be enhanced by expanding the range of bases that can form the quartet motif.

Results: Native polyacrylamide gel electrophoresis of oligonucleotides bearing runs of *iso*-G provides strong support for tetraplex formation via cation-promoted DNA strand association. In particular, when strands of different lengths bearing the same *iso*-G tetrad recognition element were combined, five bands were observed after electrophoresis, corresponding to all possible heterotetraplexes with parallel strand alignment. An analogous experiment with a mixture of strands bearing *iso*-G or G tetrad recognition domains supports the existence of mixed *iso*-G/G tetraplexes with antiparallel strand alignment at chimeric junctions. *iso*-G tetraplex and quartet structure has also been probed by a photo-crosslinking experiment, ultra-violet spectroscopy and theoretical calculations.

Conclusions: As *iso*-G and G both have a marked tendency to form tetraplexes, their tandem inclusion in genetic material may be problematic, leading to double-stranded DNA half composed of bases that have a tendency to auto-associate. The resulting density of 'selfish' bases could undermine Watson–Crick pair formation, especially in a prebiotic context devoid of enzymes. Nevertheless, the ability of *iso*-G to form mixed quartets with G may provide a basis for altering the properties of tetraplexes in the domain of artificial receptors or catalysts from *in vitro* selections.

Address: Department of Chemistry, University of California, Riverside, CA 92521, USA.

Correspondence: Christopher Switzer
E-mail: switzer@citrus.ucr.edu

Key words: *ab initio* theoretical, guanine, *iso*-guanine, quartet, tetraplex

Received: **21 August 1997**
Revisions requested: **23 September 1997**
Revisions received: **6 October 1997**
Accepted: **10 October 1997**

Chemistry & Biology December 1997, 4:899–908
http://biomednet.com/elecref/1074552100400899

Introduction

Of the two Watson–Crick hydrogen-bonding patterns in nature, it is possible to reverse only one to obtain a new pattern — that found in the G–C pair. In principle, the simplest way to realize a base pair with a reversed bonding pattern is to interchange the amino and carbonyl groups of the natural bases, yielding *iso*-G and *iso*-C (Figure 1a). The resulting *iso*-G–*iso*-C pair has been probed by polymerase copying [1], ribosomal translation [2] and duplex denaturation experiments [3]. *iso*-G exhibits relatively low fidelity in enzymatic experiments that depend on Watson–Crick base pairing [1,2]. This infidelity appears to correlate with the tendency of *iso*-G to adopt more than one tautomeric form. In the absence of enzymes, however, *iso*-G exhibits relatively high fidelity, especially against cytosine [3]. This finding raises the question of whether the alternative four-letter genetic system comprising *iso*-C, *iso*-G, C and G may be viable [3].

An issue related to Watson–Crick pair formation concerns self pairing by the component bases. The fact that G forms quartets suggests that *iso*-G might also do so because both bases share the same fundamental array of Watson–Crick donor/acceptor groups as N1-H tautomers (the tautomeric form having a hydrogen atom attached to the purine nitrogen at position 1; Figure 1b). G-rich DNA sequences capable of forming tetraplexes *in vitro* occur naturally in telomeres [4], immunoglobulin gene switch regions [5] and certain gene promoters [6]. This has fueled speculation that tetraplexes function biologically. Nucleic

Figure 1

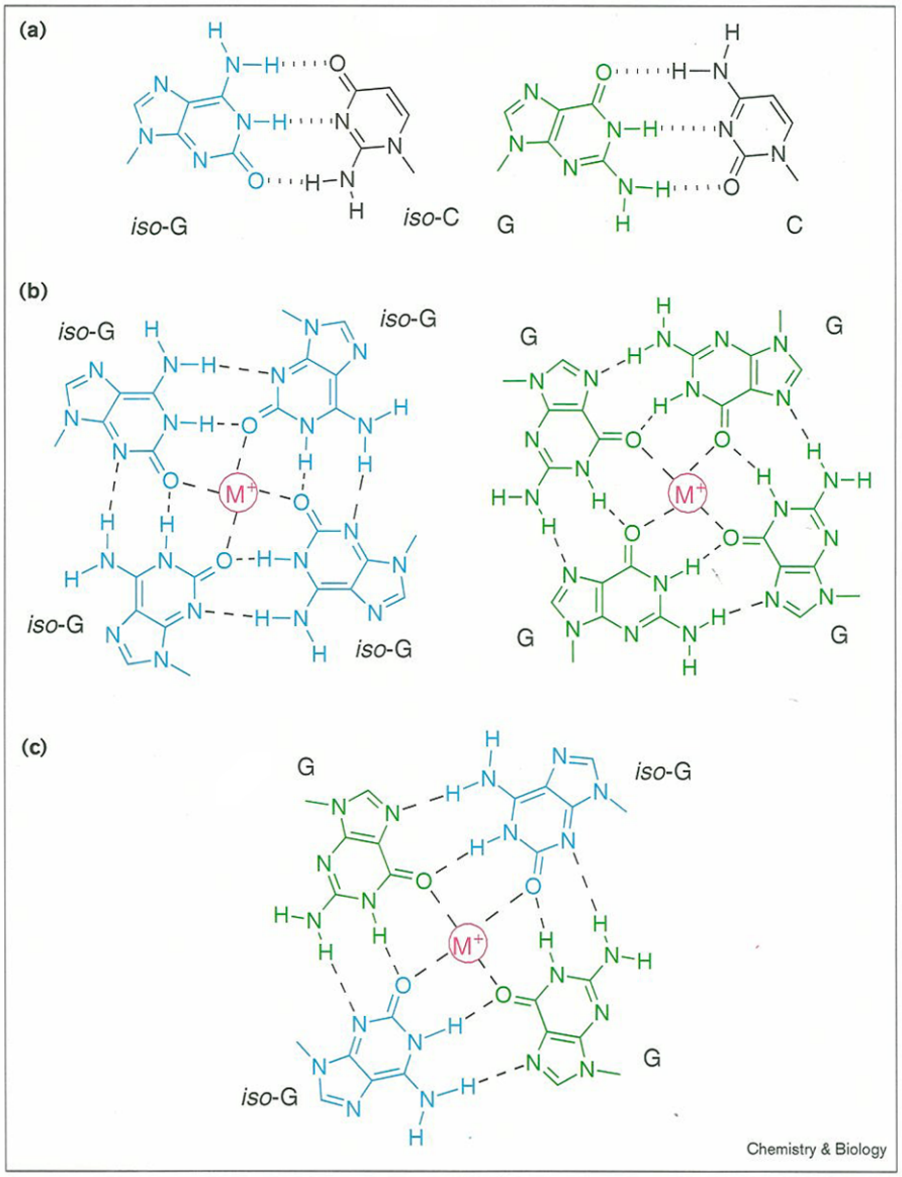

(a) *iso*-G–*iso*-C and G–C base pairs. **(b)** *iso*-G quartet model with a central monovalent cation (left); G-quartet model (right). **(c)** An example of a mixed *iso*-G/G quartet.

acid sequences that support tetraplexes are known to interfere with the non-enzymatic template-directed synthesis of oligonucleotides, however, making this structure prebiotically untenable [7]. Artificial engineering of G tetraplexes has led to biomolecular receptors [8], biomaterials [9] and catalysts [10]. The incorporation of additional bases into quartets, such as *iso*-G (Figure 1b,c), provides an opportunity to increase tetraplex diversity.

Over the past ten years, G tetraplexes have been structurally characterized by biochemical studies, nuclear magnetic resonance (NMR) and X-ray crystallography [4,11]. As a result, G tetraplexes have been determined to adopt different structures, including unimolecular, antiparallel bimolecular and parallel tetramolecular forms. An integral part of these complexes are core monovalent cations, which are positioned between adjacent quartet layers. The physical behavior of monomeric *iso*-guanosine and polymeric *iso*-guanylate is qualitatively similar to guanosine systems that form tetraplexes. *iso*-Guanosine forms gels in aqueous solution [12] that possess melting behavior similar to gels of guanosine monomers that form helical structures [13]. Poly(*iso*-G) has been suggested to associate into a four-stranded structure more stable than that of poly(G) [14,15]. Recently, Davis and coworkers [16] have reported NMR evidence for *iso*-guanosine mononucleoside aggregation to octamers in organic solvents using several different monovalent cations. Here, we assess tetraplex formation by *iso*-G-bearing oligonucleotides through native polyacrylamide gel electrophoresis (PAGE), photo-crosslinking, ultra-violet

Figure 2

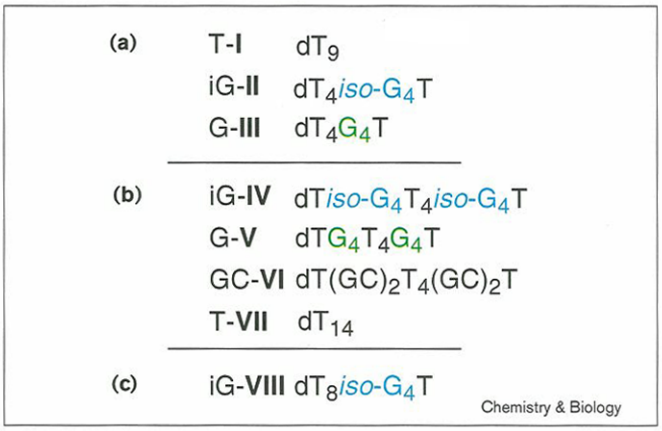

Oligodeoxynucleotides prepared in this work for the study of *iso*-G tetraplex formation. **(a)** Oligonucleotides prepared for studying the effect of a single insertion of *iso*-G or G; **(b)** oligonucleotides prepared for studying the effects of two insertions of *iso*-G or G; **(c)** oligonucleotide prepared for the study of heterotetraplexes.

(UV) spectroscopy and theoretical calculations, in both the presence and absence of sodium or potassium ions.

Results and discussion

iso-G-bearing oligomers aggregate in the presence of cations

Native PAGE has been used extensively to assay oligonucleotide association and formation of G tetraplexes in particular [17]. Two sets of oligonucleotides have been prepared to probe tetraplex formation by DNA bearing *iso*-G repeats using this method. One set incorporates a single repeat of unnatural bases and the other, two repeats (Figure 2). The first set (Figure 2a) is based on a nonamer with four contiguous *iso*-G or G bases (iG-**II** and G-**III** respectively), along with a structureless control oligomer (T-**I**). Oligomers iG-**II** and G-**III** may form tetramolecular tetraplexes as shown in Figure 3a. The second set (Figure 2b) are tetradecamers where two runs of *iso*-G or G are separated by four thymine residues (iG-**IV** and G-**V** respectively). These oligomers may associate to form bimolecular tetraplexes (Figure 3b), or tetramolecular tetraplexes (Figure 3c). Two control oligomers for this set are GC-**VI**, which forms a hairpin duplex, and T-**VII**, which is structureless (Figure 2b). Tetramolecular tetraplexes formed as shown in Figure 3a or c should have significantly reduced mobility compared to an unaggregated single strand. Similarly, bimolecular tetraplexes, shown in Figure 3b, should have reduced mobility relative to an unaggregated parent, albeit to a lesser extent than expected with tetramolecular association. Thus, comparing the mobilities of iG-**II** and iG-**IV** to those of G-**III** and G-**V** should give an indication of the degree of aggregation in the unnatural system. Results from initial native PAGE experiments are shown in Figure 4a–c. The autoradiograms depicted in these panels derive from, respectively, electrophoresis with no salt added to the running buffer (0.6 × TBE running buffer alone), added 50 mM potassium chloride and added 50 mM sodium chloride. Native gel electrophoresis under low salt conditions (Figure 4a) shows no indication of intermolecular aggregation for oligomers bearing *iso*-G or G, although the data do suggest that iG-**IV** may form a hairpin.

Dramatic changes in the native gel mobility of iG-**II** and G-**III** bearing single purine repeats are observed upon incubation and electrophoresis in the presence of potassium chloride or sodium chloride (lanes 2,3, Figure 4b,c). In the presence of potassium ions, both oligomers display bands with highly retarded but similar mobility that are completely absent under low salt conditions. Given that G-**III** has been shown to form a tetraplex in the presence of potassium ions [18], this finding is consistent with tetramolecular tetraplex formation by iG-**II**. Also notable from Figure 4b is that iG-**II** apparently yields a single tetraplex species to the exclusion of uncomplexed single strand, whereas G-**III** forms more that one tetraplex species with uncomplexed single strand remaining. This observation suggests that the *iso*-G tetraplex may be more stable than the G tetraplex in K^+, especially as the concentration of G-**III** was tenfold greater than that of iG-**II** in this experiment. Aggregation of both iG-**II** and G-**III** is less in the presence of sodium chloride (Figure 4c) than in the presence of potassium chloride, where the effect on iG-**II** is much more pronounced. In addition, G-**III** yields what appears to be a single tetraplex species in the presence of Na^+, in contrast to the result in K^+. The contrasting stability of the iG-**II** aggregate in K^+ versus Na^+ suggests a structural role for these cations, possibly at the interstices of adjacent *iso*-G quartets, analogous to their role in G quartets.

Bands with diminished mobility are also observed in high salt native gels of the double purine repeat oligomers iG-**IV** and G-**V**. In the presence of K^+, iG-**IV** appears to form a tetraplex (Figure 4b, lane 4) as judged by its mobility compared to that of GC-**VI** and T-**VII** in lanes 6 and 7. In lane 5, faint bands can be seen for G-**V** in the autoradiogram exposure represented, but longer exposure shows many bands with smearing. This observation is consistent with the known tendency of K^+ to induce multimeric parallel tetraplexes in sequences, similar to G-**V** [19]. In the presence of Na^+ rather than K^+, iG-**IV** forms a high mobility band (Figure 4c, lane 4) similar to running buffer alone (see above). In contrast, G-**V** yields a band in lane 5 of the Figure 4c with slightly diminished mobility compared to T-**VII** (lane 7). This band is most probably the antiparallel tetraplex resulting from dimerization of hairpins. Very similar mobility relationships between an unstructured marker, antiparallel hairpin dimer tetraplex and single-stranded oligomer have been reported by Kallenbach and

Figure 3

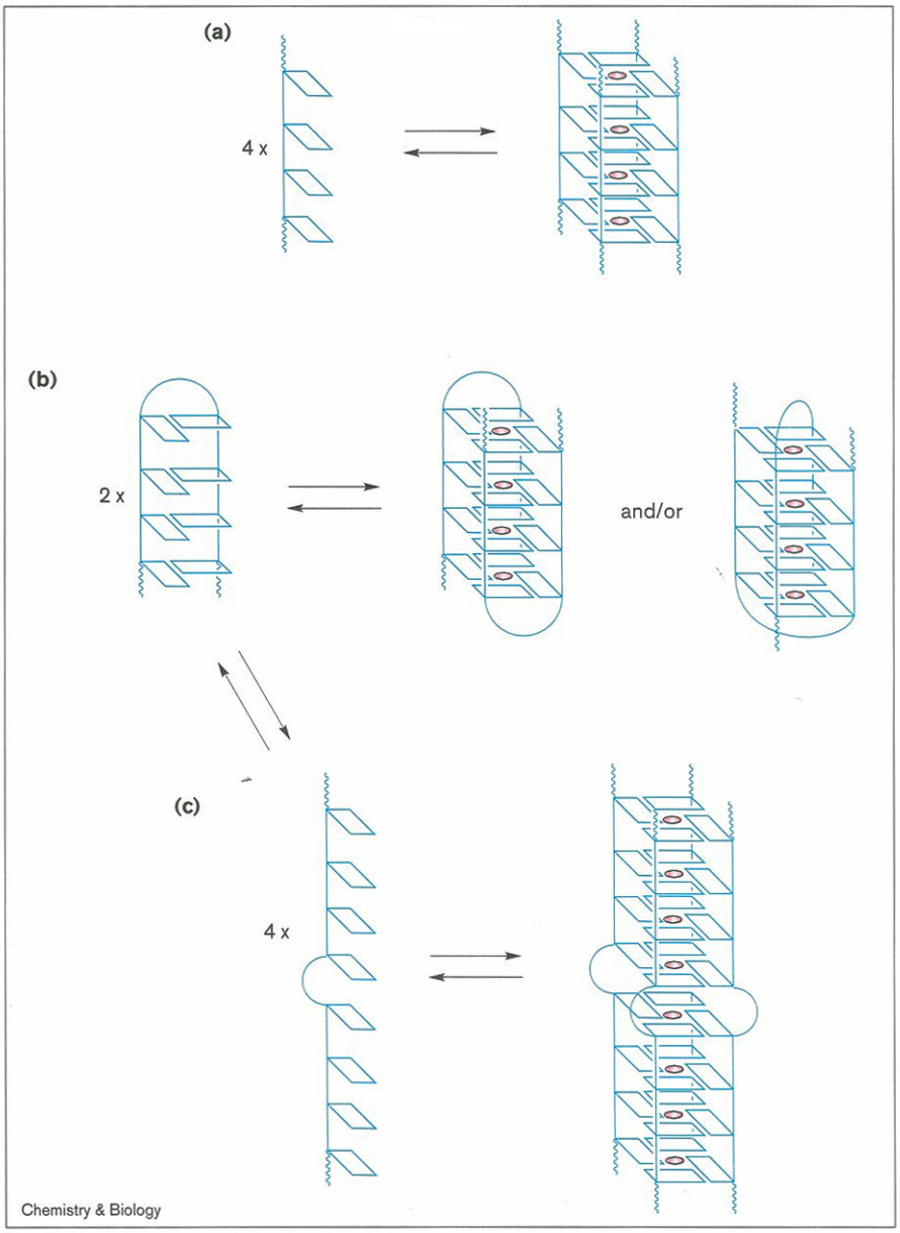

(a) The tetramolecular association that is possible with iG-**II** or G-**III**. Two competing pathways of tetraplex formation by iG-**IV** or G-**V**: bimolecular **(b)** and tetramolecular **(c)**.

coworkers [20] for $d(T_4G_4)_2$ in the presence of Na^+. Additional data reported by Kallenbach allow a prediction to be made regarding the K^+ structure of iG-**IV** (Figure 4b, lane 4) — namely, that it exists as a parallel-stranded tetramolecular tetraplex (Figure 3c), and not as a bimolecular tetraplex formed from hairpin dimers (Figure 3b). Although a coherent parallel-stranded structure is not observed for G-**V** in Figure 4b, lane 5 in the present work for the reasons noted above, a single species is observed in Kallenbach's work with $d(T_4G_4)_2$ in K^+, where the difference in mobility of his parallel-stranded tetraplex relative to a 16-mer marker is about the same as that seen with iG-**IV** in lane 4 relative to the 14-mer marker in lane 7. These observations also explain the dramatically different mobilities for the tetraplexes observed for G-**V** in Figure 4c, lane 5, relative to iG-**IV** in Figure 4b, lane 4.

Heterotetraplexes of *iso*-G demonstrate parallel-stranded tetramolecular association

Definitive evidence for *iso*-G tetraplex formation has been sought by examining the electrophoretic behavior of aggregates deriving from a mixture of iG-**II** and iG-**VIII** (Figure 5a). These oligomers have trivial charge and size differences deriving from the number of 5′-thymidylate residues (four compared to eight) but invariant *iso*-G_4 complexing domains, and are, in principle, capable of

Figure 4

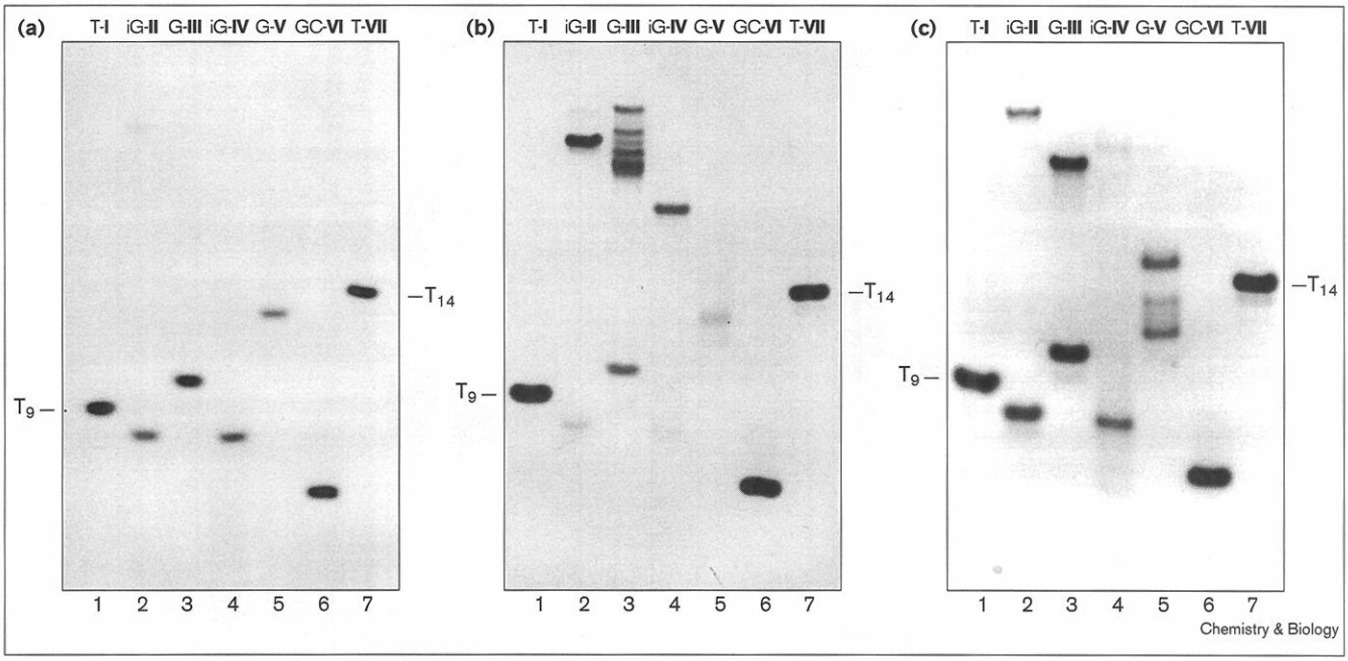

Comparison between *iso*-G and G oligonucleotide aggregates in the presence of different cations. **(a)** An autoradiogram of a native 20% polyacrylamide gel: electrophoresis was performed at 4°C with 0.6 × TBE (Tris, boric acid, EDTA) alone as the running buffer. **(b)** An autoradiogram of a native 20% polyacrylamide gel: electrophoresis was performed at 4°C with 0.6 × TBE and 50 mM potassium chloride running buffer. **(c)** An autoradiogram of a native 20% polyacrylamide gel: electrophoresis was performed at 4°C with 0.6 × TBE and 50 mM sodium chloride running buffer.

forming heterotetraplexes. Five heterotetramer bands are expected by native gel electrophoresis if parallel-stranded tetramolecular tetraplexes form (Figure 5b), whereas six bands are anticipated for antiparallel tetraplex formation

Figure 5

Characterization of *iso*-G tetraplexes. **(a)** An autoradiogram of a native 20% polyacrylamide gel: electrophoresis was performed at 4°C with 0.6 × TBE and 50 mM potassium chloride running buffer. The anticipated outcomes of parallel **(b)** and antiparallel **(c)** tetramolecular association of iG-II and iG-VIII with themselves and one another. Five complexes are predicted to be electrophoretically distinguishable in the parallel case, whereas a total of six are predicted for the antiparallel case.

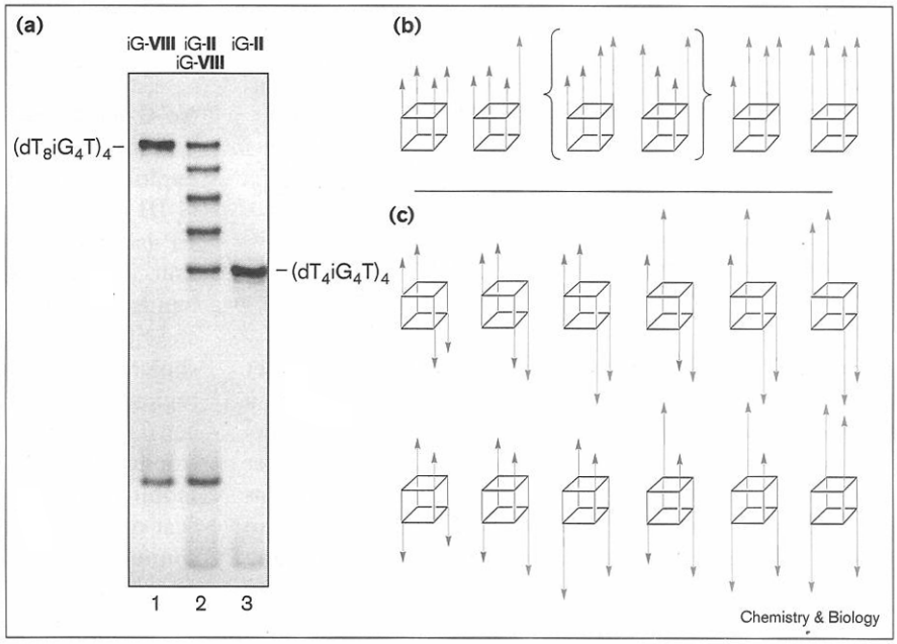

Figure 6

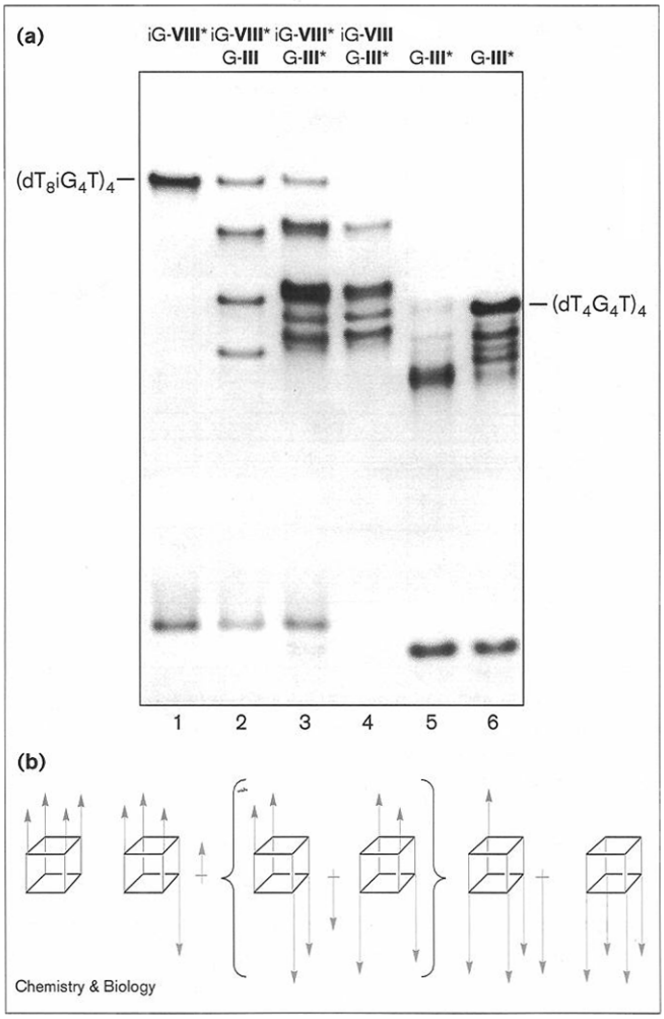

Characterization of *iso*-G and G chimeric tetraplexes. **(a)** An autoradiogram of a native 20% polyacrylamide gel: electrophoresis was performed at 4°C with 0.6 × TBE and 50 mM potassium chloride running buffer. Lane 1, [^{32}P]iG-**VIII** alone; lane 2, mixture of [^{32}P]iG-**VIII** and unlabeled G-**III**; lane 3, mixture of [^{32}P]iG-**VIII** and [^{32}P]G-**III**; lane 4, mixture of unlabeled iG-**VIII** and [^{32}P]G-**III**, lane 5, [^{32}P]G-**III** alone; lane 6, [^{32}P]G-**III** (for this lane alone the pre-incubation procedure was modified to include only a single denaturation step). **(b)** The anticipated outcome from antiparallel tetramolecular combination of iG-**VIII** and G-**III**. Five complexes are predicted to be electrophoretically distinguishable. Approximate dipole moments are shown in pink.

Figure 7

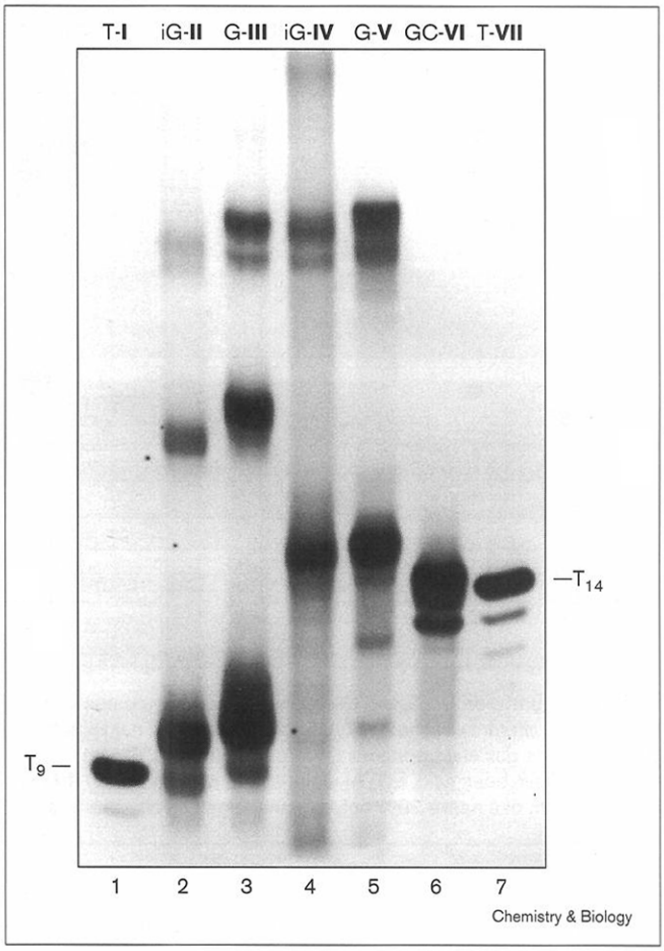

Analysis of photo-crosslinked *iso*-G and G oligonucleotide aggregates. An autoradiogram of a denaturing 20% polyacrylamide gel: electrophoresis was performed at 45°C with 1 × TBE running buffer. 5′-^{32}P-end-labelled oligonucleotides were irradiated at 253 nm as described in the Materials and methods section.

(Figure 5c) [21]. These outcomes represent the number of electrophoretically unique complexes deriving from a statistical distribution of the different length oligomers within tetramolecular tetraplexes. Observation of fewer than five bands would be inconsistent with tetramolecular association. In Figure 5a, iG-**VIII** and iG-**II** alone appear in lanes 1 and 3, and a mixture of the two in lane 2. Three new bands are present in lane 2. This outcome is fully consistent with parallel-stranded tetramolecular tetraplex formation.

iso-G and G strands combine to form chimeric tetraplexes

The formation of *iso*-G/G chimeric tetraplexes has been explored by native gel electrophoresis of iG-**VIII** and G-**III** (Figure 6a). These strands were combined in both ^{32}P-labeled and unlabeled forms to aid band identification. Three new bands are seen in addition to the two bands from the pure *iso*-G and G tetraplexes. This is the anticipated result of mixed base tetraplex formation, as shown in Figure 6b. As the number of overhanging regions on a given tetraplex face in Figure 6b are not constant through the series, non-incremental electrophoretic mobility changes are expected — a greater mobility for one of the chimeric tetraplexes compared to that of the G-**III** homotetraplex notwithstanding. In this connection, it is interesting to note that the chimeric tetraplexes should have macroscopic dipole moments as indicated. Such moments would affect the angular velocity of the tetraplexes [22], causing them to align with the

Table 1

***Ab initio* data.**

Entry		3-21G(*) $E_{SCF, rel}$ (kcal/mol)	E_{SCF} (Hartrees)	E_{int} (kcal/mol)	BSSE (kcal/mol)	E_{int}-K^+ (kcal/mol)
1	*iso*-G N1-H, K^+ tetraplex	0.00	−2741.769127	−151.1	60.0	−64.9
2	*iso*-G O2-H, K^+ tetraplex	53.5	−2741.683860	−99.3	48.2	−58.9
3	*iso*-G imino oxo, K^+ tetraplex	46.0	−2741.695778	−108.8	53.7	−69.2
4	*iso*-G N1-H tetraplex	0.00	−2145.606355	−86.2	27.0	
5	*iso*-G O2-H tetraplex	36.9	−2145.547429	−40.4	25.8	
6	*iso*-G imino oxo tetraplex	44.3	−2145.535683	−39.6	26.8	
7	*iso*-G N1-H	2.53	−536.356430			
8	*iso*-G O2-H	0.00	−536.360460			
9	*iso*-G imino oxo	1.89	−536.357450			

Reported energies are not zero point corrected. Interaction energies (E_{int}) have been corrected for basis set superposition error (BSSE), which is also separately listed. BSSE was estimated as described in the Material and methods section. E_{SCF} is the total energy of the molecule calculated at the Hartree–Fock level using the self-consistent field (SCF) method. $E_{SCF, rel}$ is the relative total energy of molecules with respect to the following three groupings of entries: 1–3, 4–6, 7–9. 1 Hartree is 627.51 kcal/mol.

electrophoretic field. Different orientations of the chimeric tetraplexes within the electrophoretic field provides an additional basis for anticipating non-linear relationships in the mobilities of these complexes.

Photo-crosslinking of tetraplexes

Further support for aggregation of iG-**II** and iG-**IV** is provided by a photo-crosslinking experiment (Figure 7). Monomer, dimer and trimer crosslinked products are apparent for iG-**II**, G-**III** and iG-**IV** (Figure 7, lanes 2–4). Monomer and dimer are apparent for G-**V** (Figure 7, lane 5). G-oligomer lanes contain slightly more material than those with *iso*-G, and, consequently, crosslinks appear slightly more intense.

A UV spectroscopic view of quartet structure

A UV spectrum of iG-**IV** in 1 M KCl shows appreciable absorbance at 290 nm (see the Supplementary material) which implicates the N1-H tautomer of *iso*-G as a component of the quartets, as this long wavelength absorbance is characteristic of the N1-H tautomer [23]. This simple analysis does not allow other tautomers to be ruled out, as overlap is anticipated between the spectrum of the thymine component and the O2-H and N3-H tautomers of *iso*-G [23], were the latter to be present as well.

Ab initio calculations on competing quartet models

Results from *ab initio* calculations at the 3-21G(*) level of theory are given in Table 1. Calculations were performed on tetramers of *iso*-G in the N1-H, O2-H and imino oxo tautomeric forms with (Figure 8) and without a central potassium ion. The N1-H and O2-H *iso*-G tautomers have been observed previously in physical studies on monomers, depending on conditions [23,24]. Although the imino oxo tautomer has not been directly observed experimentally, it is predicted to be relatively stable by *ab initio* theory [3]. C4h symmetry was imposed on the tetramers to enhance computational efficiency, and to avoid highly non-planar complexes which would most probably be inconsistent with a tetraplex of oligonucleotides. The quartet incorporating the *iso*-G N1-H tautomer is calculated to be most stable irrespective of complexation with K^+. At the same time, however, this tautomer of *iso*-G gives the least stable monomer. Interaction energies (E_{int}) were determined for the tetraplexes by subtracting energies of the isolated tetraplex components from the energy of the complex and they are listed in Table 1. The interaction energy of K^+ with the various quartets (E_{int}-K^+) has been estimated from the E_{int} of a given quartet in the presence of K^+, less the E_{int} of the quartet in the absence of K^+.

The E_{int} term suggests that quartets incorporating O2-H and imino oxo tautomers interact nearly identically in the absence of potassium, and the dissociation energy of the N1-H *iso*-G quartet is roughly twice either of these complexes. The E_{int}-K^+ term implies that quartets of all three tautomers are stabilized by potassium to roughly the same extent. Enhanced E_{int} of the N1-H *iso*-G quartet lacking a central potassium ion may derive, in part, from this motif being capable of forming bifurcated hydrogen bonds [25], which are apparent in the optimized geometry (data not shown).

The above analysis is predicated on the reasonableness of placing potassium ions in the quartet plane. It is

Figure 8

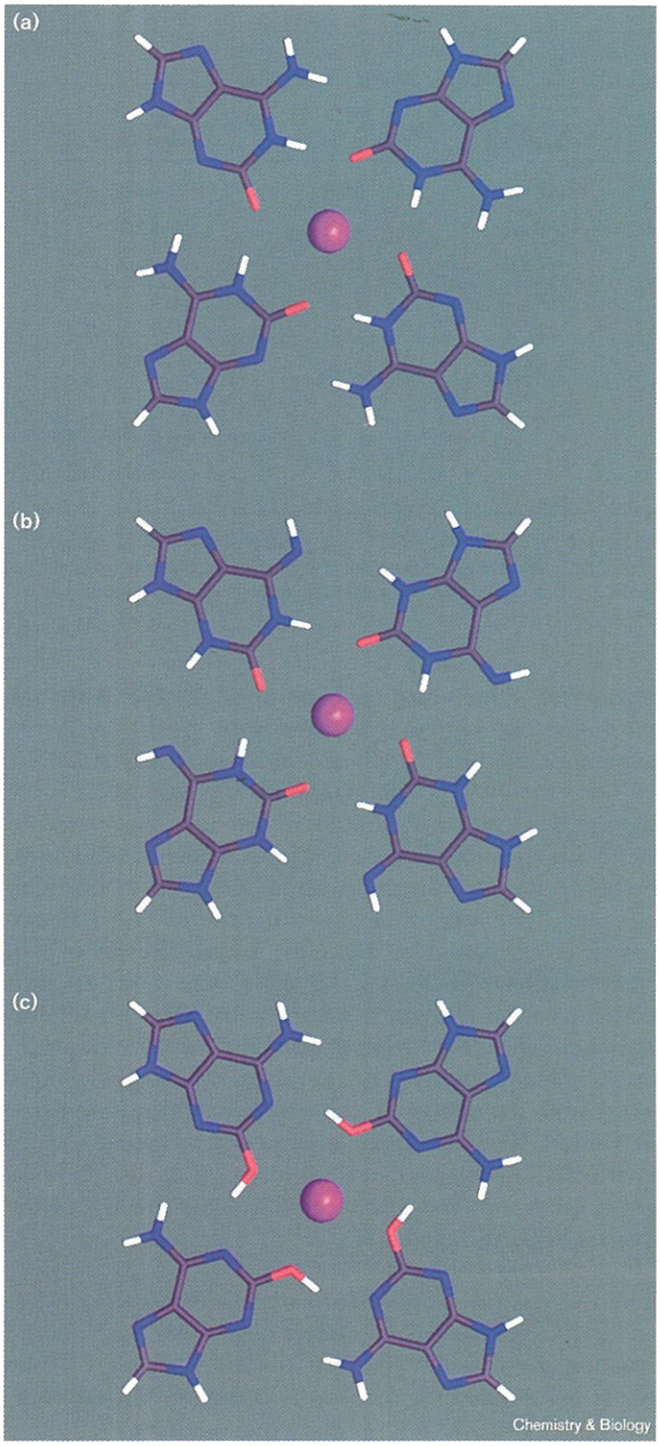

Ab initio 3-21G* optimized geometries of *iso*-G quartets with a central potassium ion incorporating **(a)** an N1-H tautomer, **(b)** an imino oxo tautomer and **(c)** an O2-H tautomer.

evident from the calculations that doing so is not entirely unreasonable, as in all three instances investigated such ion placement was stabilizing. Nonetheless, it is generally assumed that sodium or potassium ions will adopt an octahedral geometry in tetraplexes where they reside at the interstitial region between quartets. This is partially confirmed by an X-ray crystallographic study of the potassium form of telomeric DNA [26], although when low resolution data from this study were analyzed, electron density tended to smear between the region that defines adjacent quartet planes. In a different X-ray crystallographic study it was observed that while sodium ions at the center of a tetraplex were octahedral, a gradual displacement of the ions toward square planar geometry occurred on moving to the ends of the structure [27]. Thus, for sodium ions, both coordination geometries are relevant. Our results suggest this could also be true for potassium ions.

Quartet overview

The *iso*-G quartet shown in Figure 1b is consistent with all of the present data. UV spectroscopic data support the *iso*-G N1-H tautomeric form. Native gel experiments show a profound structural dependence on monovalent cation type, in keeping with a metal ion core. In addition, the viability of the quartet structure is supported by theoretical calculations. This quartet model was first discussed by Davis *et al.* [28] in connection with cation-promoted aggregation of *iso*-guanosine in organic solvents.

One example of extending the *iso*-G quartet model to include mixed *iso*-G and G quartets is shown in Figure 1c (the three other structures include a 1:3 complex and a 3:1 complex, and are given in the Supplementary material). This is accomplished easily as quartets of pure N1-H *iso*-G and pure G are based on the same donor–donor hydrogen-bonding pattern, and on metal ion coordination by centrally located carbonyl groups. This model has been invoked in recent work by Seela *et al.* [15] where mixed aggregates of $T_4G_4T_4$ and T_4*iso*-G_4T_4 were observed in ion exchange chromatographic traces.

Tetraplex overview

Homogenous *iso*-G tetraplexes behave differently from G tetraplexes in several important respects. First, they appear to be less stabilized by Na^+ and relatively more stabilized by K^+. The trend of enhanced stabilization by K^+ over Na^+, however, is the same for both tetraplexes. It has been pointed out that the main factor for K^+ selectivity originates from differences in free energies of hydration for the two ions [29]. Second, homogenous *iso*-G tetraplexes would appear to occur only in parallel form. Parallel-stranded *iso*-G tetraplexes should bear all *anti* conformations about glycosidic bonds. The alternative *syn* conformation of *iso*-G directs both of the quartet hydrogen-bond acceptor atoms towards the deoxyribose ring where, for steric reasons, they are relatively unavailable for pairing. Bimolecular or unimolecular antiparallel tetraplexes require both *syn* and *anti* base orientations, and consequently these structures would seem only a

formal possibility for *iso*-G. Bimolecular foldback G tetraplexes may be the basis for chromosomal dimerization during interphase [4,30]. Parallel G tetraplexes may be the mechanism for association of pairs of sister chromatids during meiosis [4,5,30]. If future studies confirm that homogeneous *iso*-G tetraplexes may only align in parallel, their ability to mimic only the latter (hypothetical) function of G tetraplexes is another point of divergence. An inability to form foldback tetraplexes could be advantageous prebiotically, nonetheless, because tetraplex formation by isolated polynucleotide templates would be rendered improbable.

Significance

Tetraplexes, like duplexes and triplexes, organize nucleic acids three dimensionally, but they have also been shown to be important in the organization of *in vitro* selected receptors and catalysts. Additional quartet motifs incorporating *iso*-guanine (*iso*-G) provide a potential avenue by which tetraplex diversity may be enhanced, possibly leading to improvements in their functional characteristics. We have established here that runs of *iso*-G not only provide a basis for tetramolecular DNA strand association, but, moreover, for tetramolecular strand association with a stability that rivals or surpasses that of their guanine counterparts. Thus, *iso*-G has the potential to impart favorable characteristics to tetraplexes, including combinatorial diversity through the formation of at least three different kinds of mixed quartet with G. The fact that *iso*-G and G in quartets are both self complementary and mutually complementary could lead to the development of a tetraplex 'genetic code' by the creation of additional bases with different quartet motifs.

Materials and methods

iso-G phosphoramidite and oligonucleotide synthesis

Synthesis of suitably protected 2'-deoxy-*iso*-guanosine phosphoramidite as well as natural and modified oligonucleotides was performed as described [3].

Polyacrylamide gel assays of tetraplex formation

Oligonucleotide (400 pmol, except in the case of G-III where 4000 pmol was used) was combined in an Eppendorf tube with 1 µl 10× kinase buffer (700 mM Tris-HCl pH 7.6, 100 mM $MgCl_2$, 50 mM DTT), 1 µl [γ-^{32}P]ATP (1 µCi), 4 µl H_2O, and 1 µl T4 polynucleotide kinase (30 U, US Biochemicals). The sample was incubated for 30 min at 37°C, after which 1 µl 660 µM ATP was added. After incubation for an additional 30 min at 37°C, 10 µl 500 mM KCl or NaCl (or simply 10 µl pure H_2O in the case of the 'no salt' experiment) was added, the sample heated at 90°C for 10 min, centrifuged, and then incubated at 4°C for 24 h. Electrophoresis of samples (10 µl) was on a native 20% polyacrylamide gel kept at 4°C. Running buffer contained either 50 mM KCl, 50 mM NaCl, or no additional salt, along with 0.6× TBE (Tris, boric acid, EDTA pH 8.6) where the pH of the buffer was adjusted with hydroxide of the appropriate counterion. After electrophoresis, the gels were exposed to film for 0.5–2 h. UV crosslinking experiments were accomplished by irradiating 10 µl of a tetraplex solution after it had been incubated for 24 h at 4°C with a low pressure mercury lamp. Electrophoresis of the samples was performed on a denaturing (7 M urea) 20% polyacrylamide gel.

Polyacrylamide gel assays of mixed tetraplex formation

Oligonucleotides (400 pmol each) were transferred to Eppendorf tubes, lyophilized, and combined with 6 µl H_2O, 1 µl 10× kinase buffer (100 mM Tris-HCl pH 7.6, 100 mM $MgCl_2$, 50 mM DTT), 1 µl [γ-^{32}P] ATP (1 µCi), and 1 µl T4 polynucleotide kinase (30 U, US Biochemical). The samples were incubated for 30 min at 37°C, and then 1 µl 660 µM ATP was added, and incubation was continued for an additional 30 min at 37°C. A portion of kinased oligonucleotide (3.75 µl, 150 pmol) was then transferred to separate Eppendorf tubes, and combined with unkinased oligonucleotide (150 pmol) as necessary, and enough H_2O to give a final reaction volume of 20 µl. The reaction mixture was heated for 10 min at 90°C, followed by the addition of 5 µl 2 M KCl, and then heated for an additional 10 min at 90°C. Upon cooling to room temperature, the mixture was centrifuged and stored for 24 h at −20°C. Electrophoresis of samples (10 µl) was on a native 20% polyacrylamide gel at 4°C with 0.6 × TBE running buffer containing 50 mM KCl.

UV spectroscopy

UV spectra were recorded on a Hewlett-Packard 8452a diode-array spectrophotometer.

Ab initio *calculations*

Basis set superposition errors (BSSE) were estimated by the counterpoise method [31]. Specifically, this error was estimated from monomer energies for (1) iso-G (E_{iG}, using the geometry assumed in a complex) and (2) K^+ (E_K), and counterpoise calculations of (1) *ABCD[K+]* (E_{iG^*}), and (2) *[ABCDK+]* (E_{K^*}), where italics correspond to ghost orbital regions and items between square brackets only pertain to complexes bearing potassium. The estimation of BSSE is derived from: BSSE (CP) = 4 ($E_{iG} - E_{iG^*}$) + [$E_K - E_{K^*}$]. Calculations were performed on a Cray C98/8128 at the San Diego Supercomputer Center using Gaussian 94 [32].

Supplementary material

A UV spectrum of iG-IV in 1 M KCl and further *iso*-G quartet models are published with this paper on the internet.

Acknowledgements

This work was supported by grants from NASA (NAGW-4184) and the National Institutes of Health (GM 47375).

References

1. Switzer, C., Moroney, S.E. & Benner, S.A. (1989). Enzymatic incorporation of a new base pair into DNA and RNA. *J. Am. Chem. Soc.* **111**, 8322-8323.
2. Bain, J.D., Switzer, C., Chamberlin, A.R. & Benner, S.A. (1992). Ribosome-mediated incorporation of a non-standard amino acid into a peptide through expansion of the genetic code. *Nature* **356**, 537-539.
3. Roberts, C., Bandaru, R., & Switzer, C. (1997). Theoretical and experimental study of iso-guanine and iso-cytosine: base pairing in an expanded genetic system. *J. Am. Chem. Soc.* **20**, 4640-4649.
4. Rhodes, D. & Giraldo, R. (1995). Telomere structure and function. *Curr. Opin. Struct. Biol.* **5**, 311-322.
5. Sen, D. & Gilbert, W. (1988). Formation of parallel four-stranded complexes by guanine-rich motifs in DNA and its implications for meiosis. *Nature* **334**, 364-366.
6. Murchie, A.I.H. & Lilley, D.M.J. (1992). Retinoblastoma susceptibility genes contain 5' sequences with a high propensity to form guanine-tetrad structures. *Nucleic Acids Res.* **20**, 49-53.
7. Rembold, H. & Orgel, L.E. (1994). Single-strand regions of Poly(G) act as templates for Oligo(C) synthesis. *J. Mol. Evol.* **38**, 205-210.
8. Paborsky, L.R., McCurdy, S.N., Griffin, L.C., Toole, J.J. & Leung, L.L. (1993). The single-stranded DNA aptamer-binding site of human thrombin. *J. Biol. Chem.* **268**, 20808-20811.
9. Marsh, T.C., Vesenka, J. & Henderson, E. (1995). A new DNA nanostructure, the G-wire, imaged by scanning probe microscopy. *Nucleic Acids Res.* **23**, 696-700.
10. Li, Y. & Sen, D. (1996). A catalytic DNA for porphyrin metallation. *Nat. Struct. Biol.* **3**, 743-747.

11. Williamson, J.R. (1994). G-Quartet structures in telomeric DNA. *Annu. Rev. Biophys. Biomol. Struct.* **23**, 703-730.
12. Ravindranathan, R.V. & Miles, H.T. (1965). Helix formation by isoguanosine. *Biochim. Biophys. Acta* **94**, 603-606.
13. Sasisekharan, V., Zimmerman, S. & Davies, D.R. (1975). The structure of helical 5′-guanosine monophosphate. *J. Mol. Biol.* **92**, 171-179.
14. Golas, T., Fikus, M., Kazimierzuk, Z. & Shugar, D. (1976). Preparation and properties of an analogue of Poly(A) and Poly(G): Poly(Isoguanylic Acid). *Eur. J. Biochem.* **65**, 183-192.
15. Seela, F., Wei, C.F. & Melenewski, A. (1996). Isoguanine quartets formed by $d(T_4isoG_4T_4)$: tetraplex identification and stability. *Nucleic Acids Res.* **24**, 4940-4945.
16. Tirumala, S. & Davis, J.T. (1997). Self-assembled ionophores. An isoguanosine-K^+ octamer. *J. Am. Chem. Soc.* **119**, 2769-2776.
17. Williamson, J.R., Raghuraman, M.K. & Cech, T.R. (1989). Monovalent cation-induced structure of telomeric DNA: the G-quartet model. *Cell* **59**, 871-880.
18. Lu, M., Guo, Q. & Kallenbach, N.R. (1992). Structure and stability of sodium and potassium complexes of dT_4G_4 and dT_4G_4T. *Biochemistry* **31**, 2455-2459.
19. Marsh, T.C. & Henderson, E. (1994). G-Wires: self-assembly of a telomeric oligonucleotide, d(GGGGTTGGGG), into large superstructures. *Biochemistry* **33**, 10718-10724.
20. Guo, Q., Lu, M. & Kallenbach, N.R. (1993). Effect of thymine tract length on the structure and stability of model telomeric sequences. *Biochemistry* **32**, 3596-3603.
21. Kim, J., Cheong, C. & Moore, P.B. (1991). Tetramerization of an RNA oligonucleotide containing a GGGG sequence. *Nature* **351**, 331-332.
22. Fair, M.C. & Anderson, J.L. (1989). Electrophoresis of nonuniformly charged ellipsoidal particles. *J. Colloid Interface Sci.* **127**, 388-400.
23. Sepiol, J., Kazimierczuk, Z. & Shugar, D. (1976). Tautomerism of isoguanosine and solvent-induced keto-enol equilibrium. *Z. Naturforsch* **31**, 361-370.
24. Seela, F., Wei, C.F. & Kazimierczuk, Z. (1995). Substituent reactivity and tautomerism of isoguanosine and related nucleosides. *Helv. Chim. Acta* **78**, 1843-1854.
25. Czerminski, R., Szczepaniak, K., Person, W.B. & Kwiatkowski, J.S. (1990). Intermolecular interactions and tautomerism of nucleic acid bases and their analogues. *J. Mol. Struct.* **237**, 151-163.
26. Kang, C.-H., Zhang, X., Ratliff, R., Moyzis, R. & Rich, A. (1992). Crystal structure of four-stranded Oxytricha telomeric DNA. *Nature* **356**, 126-131.
27. Laughlan, G., *et al.*, & Luisi, B. (1994). The high resolution crystal structure of a parallel-stranded guanine tetraplex. *Science* **265**, 520-524.
28. Davis, J.T., Tirumala, S., Jenssen, J.R., Radler. & Fabris, D. (1995). Self-assembled ionophores from isoguanosine. *J. Org. Chem.* **60**, 4167-4176.
29. Hud, N.V., Smith, F.W., Anet, F.A.L. & Feigon, J. (1996). The selectivity for K^+ versus Na^+ in DNA quadruplexes is dominated by relative free energies of hydration: a thermodynamic analysis by ^1H NMR. *Biochemistry* **35**, 15383-15390.
30. Miura, T. & Thomas, G.J. (1994). Structural polymorphism of telomere DNA: interquadruplex and duplex-quadruplex conversions probed by raman spectroscopy. *Biochemistry* **33**, 7848-7856.
31. Turi, L. & Dannenburg, J.J. (1993). Correcting for basis set superposition error in aggregates containing more than two molecules: ambiguities in the calculation of the counterpoise correction. *J. Phys. Chem.* **97**, 2488-2490.
32. Frisch, M. J., *et al.*, & Pople, J.A. (1995). Gaussian 94, Revision B.1, Gaussian Inc., Pittsburgh, PA.